Available online at www.sciencedirect.com
SCIENCE DIRECT®
Bioorganic & Medicinal Chemistry 14 (2006) 1143–1159
Bioorganic & Medicinal Chemistry

High-throughput screening of ecdysone agonists using a reporter gene assay followed by 3-D QSAR analysis of the molting hormonal activity

Craig E. Wheelock,[a,b,†] Yoshiaki Nakagawa,[a,*,†] Toshiyuki Harada,[a] Nobuhiro Oikawa,[a] Miki Akamatsu,[c] Guy Smagghe,[d] Dimitra Stefanou,[e] Kostas Iatrou[e] and Luc Swevers[e]

[a]*Division of Applied Life Sciences, Graduate School of Agriculture, Kyoto University, Kyoto 606-8502, Japan*
[b]*Bioinformatics Center, Institute for Chemical Research, Kyoto University, Uji 611-0011, Japan*
[c]*Division of Environmental Science and Technology, Graduate School of Agriculture, Kyoto University, Kyoto 606-8502, Japan*
[d]*Laboratory of Agrozoology, Department of Crop Protection, Faculty of Bioscience Engineering, Ghent University, Coupure Links 653, B-9000 Ghent, Belgium*
[e]*Insect Molecular Genetics and Biotechnology Group, Institute of Biology, National Center for Scientific Research 'Demokritos', Aghia Paraskevi, 153 10 Athens, Greece*

Received 21 July 2005; revised 13 September 2005; accepted 14 September 2005
Available online 24 October 2005

Abstract—In this study, 172 diacylhydrazine analogs were examined for their ability to activate an ecdysone (molting hormone)-dependent reporter gene in a silkworm (*Bombyx mori*) cell-based high-throughput screening assay. The measured EC_{50} values (concentration required to cause an effect in 50% of the cells) were used to construct a 3-D QSAR model that describes the ecdysone agonist activities of the diacylhydrazine analogs. Of these compounds, 14 exhibited no activity and were excluded from the 3-D QSAR analysis. The resulting equation described ~74% of the activity for 158 compounds. The final equation consisted of 42% electrostatic and 58% steric effects ($r^2 = 0.74$ and $q^2 = 0.45$). Comparative molecular field analysis (CoMFA) was used to visualize the steric and electrostatic potential fields that were favorable and unfavorable for biological activity. Of particular interest was the observation that the hydrophobic parameter ($\log P$) was not necessary for describing the observed activities, although previous studies have cited the importance of hydrophobic parameters in both classical and 3-D QSAR analyses of these compounds. Modeling studies of the *B. mori* ecdysone receptor supported the observed physicochemical parameters required for activity reported by the CoMFA models. Comparison of the present analysis with those performed using other lepidopteran assay systems evidenced a high degree of correlation ($r^2 = 0.81$ for a Sf-9 cell-based assay and $r^2 = 0.89$ for a *Chilo suppressalis* integument-based assay), indicating that it is valid to compare the results generated with the *B. mori* cell-based system to those generated with previous lepidopteran assays. This novel assay system is amendable to a high-throughput screening format and should greatly increase our ability to discover novel agonists of molting hormone (ecdysone) activity.

1. Introduction

Insect molting and metamorphosis are regulated by the steroidal molting hormone 20-hydroxyecdysone (20E).[1] The hormone receptor consists of the ecdysone receptor (EcR) and the ultraspiracle (USP), which together form a heterodimer.[2,3] Following binding of the ligand, the 20E-EcR–USP complex activates transcription through binding to DNA target sites known as ecdysone response elements (EcREs), which are located upstream of multiple genes that are involved in molting and metamorphosis.[4] External administration of excessive doses of molting hormone-active compounds induces premature molting in larvae leading to death.[5] This observation has led to the development of a number of compounds designed to target this receptor and exert insecticidal properties.[6–9] This nuclear hormone receptor is not present in mammals and therefore represents a logical target for insecticide development.[10,11]

Keywords: *Bombyx mori*; Ecdysone receptor; Ecdysone agonists; High-throughput screening; 3-D QSAR.
* Corresponding author. Tel.: +81 75 753 6117; fax: +81 75 753 6123; e-mail: naka@kais.kyoto-u.ac.jp
† These authors contributed equally to this work.

0968-0896/$ - see front matter © 2005 Elsevier Ltd. All rights reserved.
doi:10.1016/j.bmc.2005.09.034

N-tert-Butyl-*N*,*N*′-dibenzoylhydrazine and its analogs are non-steroidal ecdysone agonists that, via binding to the EcR–USP complex, cause incomplete molting in insects leading to death. The insecticidal properties of *N-tert*-butyl-*N*,*N*′-dibenzoylhydrazine were first discovered by Wing et al., who reported that the compound RH-5849 (**1** in Table 1) was an ecdysone agonist.[12,13] Since then, a number of studies have examined the range of activities surrounding this class of compounds and structure–activity relationships have been extensively investigated.[14–21] This work has led to the release of a number of commercial products including tebufenozide,[22–24] methoxyfenozide,[25–27] chromafenozide, and halofenozide.[6,28,29] Even though all insects use 20E as a natural molting hormone, their susceptibility to non-steroidal ecdysteroid agonists exhibits species-specific variation. Insect order-specific potency was observed with halofenozide and RH-5849, which have greater activity towards coleopteran pests such as the Colorado potato beetle *Leptinotarsa decemlineata*,[30] and chromafenozide, tebufenozide, and methoxyfenozide which have extremely low potency toward coleopterans.[22] However, chromafenozide, tebufenozide and methoxyfenozide are highly toxic to lepidopteran pests such as the rice stem borer *Chilio suppressalis*[17] and the beet armyworm *Spodoptera exigua*.[31] In addition, these compounds are all ineffective against hemipterans (which includes beneficial predatory insects such as *Geocoris punctipes* and *Orius insidiosus*).[32]

The newer generation analogs discussed above have decreased mammalian toxicity relative to the initial analogs reported.[33] Our understanding of the mechanism of action of these compounds was further complicated by structural analysis of the EcR–USP heterodimer, which showed that the region of the complex that binds a strong agonist with ecdysteroidal structure (ponasterone A, Pon A) did not overlap with any of the regions that bind the non-ecdysteroidal dibenzoylhydrazines (BYI06830, a chromafenozide analog).[34] These findings suggest that even though both compounds target the same receptor, they exhibit their biological activity through different mechanisms. These results have initiated renewed interest in structure–activity relationships in an attempt to understand the mechanism by which these compounds exert their insecticidal effects. The utility of these compounds and their insecticidal properties as well as the structural selectivity exhibited by the different commercial analogs currently available has led to a number of structure and function studies as described above. However, a disadvantage of many of these studies is that they employ in vitro assay systems or time-consuming and costly radiometric assays. Swevers et al. recently described a *Bombyx mori* (silkmoth; *Lepidoptera*) cell-based high-throughput screening system for detecting ecdysteroid agonists and antagonists using synthetic compound libraries as well as plant extracts.[35] The high-throughput system is based on transformed *Bombyx*-derived Bm5 tissue culture cells that have an ecdysone-inducible green fluorescent protein (GFP) reporter cassette incorporated into their genomes. The addition of 20E at 100 nM to 1 μM quantities results in 500- to 2000-fold stimulation of GFP reporter gene activity, which can be easily quantified in individual microplate wells using a fluorescence plate reader. In comparison with other systems that detect ecdysteroid activities, the cell-based system has the advantage of being extremely rapid and robust, and by being cell-based it encompasses the necessity of crossing cellular membranes to exert biological activity. In this project, we present the first extended 3-D QSAR analysis of diacylhydrazines using this novel assay system. We measured the activity of 172 diacylhydrazine derivatives and developed a 3-D QSAR model using comparative molecular field analysis (CoMFA) to analyze the parameters that were beneficial for insecticidal activity. These effects were then further examined through a series of modeling studies performed with the *B. mori* EcR binding pocket. Results were compared to the CoMFA fields to provide a comprehensive description of agonist binding and suggest potential new agonists.

2. Results

2.1. Molting hormonal activity

The hormonal activities of 133 compounds are listed in Table 1. These compounds all have the basic dibenzoylhydrazine backbone containing an *N-tert*-butyl moiety, varying only by their substitution on the A- and B-rings (see Fig. 1 for A-ring and B-ring nomenclature). Among the 133 different dibenzoyl-type compounds tested, the commercially available compound tebufenozide (**107**) was the most potent. Another *Lepidoptera*-selective commercial insecticide, methoxyfenozide (**117**), was five times less potent than tebufenozide. Compound **109** containing an *i*-propyl group at the *para*-position of the B-ring was nearly equipotent to tebufenozide, which contains a *para*-ethyl group on the B-ring. RH-5849 (**1**) and halofenozide (**133**) were 350-fold and 70-fold less potent than tebufenozide, respectively. A total of seven compounds, **10**, **12**, **13**, **31**, **32**, **82**, and **100**, were inactive.

The activities of 21 compounds (**134**–**154**) in which one of the benzene rings was replaced by a variety of steric groups (i.e., long-chain alkyl and naphthyl) are listed in Table 2. Compound **144**, which contains an α-naphthyl group on the A-ring, was the most potent among these derivatives. However, **144** was still 10-fold less potent than the corresponding 3,5-dimethyl benzoyl analog, tebufenozide (**107**). Interestingly, compound **138**, which contained an *i*-hexyl instead of a naphthyl group, was inactive.

The bridge moiety of the compound backbone was modified as shown in Table 3 for compounds **155**–**172**. Replacement of the *tert*-butyl group with a CH_3 (**155**) or ethyl (**156**) resulted in a loss of biological activity. Substitution with a *tert*-amyl group (**162**) was slightly favored, with this compound exhibiting the greatest potency of this set of analogs. Compound **162** was also more potent than its *tert*-butyl analog compound **1** (pEC_{50} = 6.81 vs 6.37, respectively). However, **162** was still 2 orders of magnitude less potent

Table 1. Activity of *tert*-butyl-containing dibenzoylhydrazine congeners with various substituents on the A and B-rings

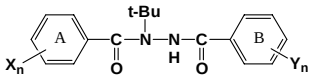

Compound	A-ring	B-ring	Activity (pEC_{50}, M)			Log *P*[b]
			Observed		Calculated[a]	
			pEC_{50}	95% CI	pEC_{50}	
1[c]	H	H	6.37	5.79–6.81	6.60	2.45[d]
2	2-F	H	6.51	5.65–7.33	5.96	2.38[d]
3	2-Cl	H	7.12	6.94–7.31	6.35	2.59[d]
4	2-Br	H	6.77	6.47–7.19	6.40	2.69[d]
5	2-I	H	6.98	6.67–7.30	6.71	2.83[d]
6	2-CF_3	H	6.20	5.91–6.50	6.06	2.85[d]
7	2-NO_2	H	6.65	6.28–7.01	6.62	2.27[d]
8	2-CH_3	H	6.65	6.46–6.83	5.94	2.75[d]
9	2-Et	H	6.23	6.06–6.40	6.15	2.96[d]
10	2-Ph	H	<4.00	—	5.12	3.89[e]
11	2-OCH_3	H	6.28	6.07–6.49	6.05	2.04[d]
12	2-O-*sec*Bu	H	<4.00	—	6.16	3.18[e]
13	2-OCH_2Ph	H	<4.00	—	6.62	3.66[e]
14	2-SCH_3	H	6.07	5.88–6.25	6.19	2.60[d]
15	3-F	H	6.68	6.43–6.84	6.30	2.78[d]
16	3-Cl	H	6.94	6.69–7.18	6.59	3.28[d]
17	3-Br	H	6.29	6.02–6.56	6.34	3.49[d]
18	3-I	H	6.15	5.85–6.44	6.58	3.72[d]
19	3-CF_3	H	5.74	5.53–5.96	5.70	3.61[d]
20	3-NO_2	H	5.13	4.93–5.33	6.07	2.73[d]
21	3-CN	H	5.82	5.61–6.02	6.03	2.34[d]
22	3-CH_3	H	7.07	6.84–7.30	6.81	2.79[d]
23	4-F	H	6.65	6.41–6.89	6.02	2.85[d]
24	4-Cl	H	6.78	6.62–6.95	6.17	3.42[d]
25	4-Br	H	6.10	5.81–6.40	5.91	3.66[d]
26	4-I	H	4.88	4.46–5.30	5.82	3.78[d]
27	4-CF_3	H	4.83	4.48–5.18	4.73	3.77[d]
28	4-NO_2	H	4.69	4.49–4.89	5.40	2.63[d]
29	4-CN	H	4.67	4.34–5.01	4.98	2.50[d]
30	4-CH_3	H	5.45	5.17–5.72	6.00	2.99[d]
31	4-*t*-Bu	H	<4.00	—	5.25	4.11[e]
32	4-Ph	H	<4.00	—	5.23	4.24[e]
33	4-OCH_3	H	4.72	4.55–4.90	5.99	2.56[d]
34	4-$O(CH_2)_3$Ph	H	4.36	4.07–4.65	4.02	4.50[e]
35	2,3-Cl_2	H	5.04	4.64–5.44	5.61	3.41[d]
36	2-CH_3-3-Cl	H	5.84	5.62–6.07	5.58	3.57[d]
37	2,3-$(CH_3)_2$	H	5.89	5.71–6.07	6.18	3.10[d]
38	2,4-Cl_2	H	6.93	6.78–7.08	5.71	3.55[d]
39	2,4-$(CH_3)_2$	H	6.24	6.05–6.43	5.77	3.18[d]
40	2,5-$(CH_3)_2$	H	5.48	5.24–5.72	6.44	3.25[d]
41	2-OCH_3-5-*n*-Pr	H	6.00	5.76–6.24	6.42	3.32[e]
42	2,6-F_2	H	5.36	5.17–5.55	5.90	2.16[d]
43	2-F-6-Cl	H	5.59	5.36–5.83	5.97	2.34[d]
44	3,4-$(CH_3)_2$	H	6.14	5.99–6.29	6.07	3.34[d]
45	3,4-$(OCH_3)_2$	H	4.33	4.10–4.67	4.85	2.09[d]
46	2,3,4-Cl_3	H	4.64	4.47–4.82	5.37	4.39[e]
47	3,5-$(CH_3)_2$	H	7.16	7.00–7.31	6.81	3.39[d]
48	2,5-Cl_2-3-CF_3	H	5.40	5.07–6.03	5.27	4.68[e]
49	2-OCH_3-3,5-$(CH_3)_2$	H	5.34	5.15–5.54	6.25	2.91[e]
50	2,3,4,5-F_4	H	6.67	6.46–6.88	5.68	3.44[d]
51	2,3,4,5,6-F_5	H	4.34	4.18–4.50	5.50	3.25[d]
52	2-Cl	2-F	7.29	7.25–7.50	6.63	2.63[d]
53	2-Cl	2-Cl	6.48	6.26–6.70	6.62	2.75[d]
54	2-Cl	2-Br	6.50	6.28–6.73	6.03	2.91[f]
55	2-Cl	2-I	5.89	5.72–6.07	6.46	3.11[f]
56	2-Cl	2-CF_3	5.76	5.48–6.03	5.93	3.02[f]
57	2-Cl	2-NO_2	6.21	5.97–6.45	5.81	1.99[f]
58	2-Cl	2-CH_3	7.14	6.89–7.40	6.25	2.91[d]
59	2-Cl	2-Ph	4.58	4.25–4.91	5.18	3.77[f]

(*continued on next page*)

Table 1 (*continued*)

Compound	A-ring	B-ring	Activity (pEC_{50}, M)			Log *P*[b]
			Observed		Calculated[a]	
			pEC_{50}	95% CI	pEC_{50}	
60	2-Cl	2-OCH_3	5.21	4.61–5.80	6.02	2.37[f]
61	2-Cl	2-SCH_3	6.17	5.99–6.36	6.01	2.84[f]
62	2-Cl	3-F	7.16	6.99–7.33	5.87	2.88[d]
63	2-Cl	3-Cl	6.81	6.62–7.00	6.53	3.49[d]
64	2-Cl	3-Br	6.72	6.42–7.02	6.45	3.62[f]
65	2-Cl	3-I	6.20	6.03–6.35	6.73	3.87[f]
66	2-Cl	3-CF_3	6.03	5.60–6.45	6.30	3.70[f]
67	2-Cl	3-NO_2	5.70	5.43–5.96	6.25	2.73[f]
68	2-Cl	3-CN	6.02	5.88–6.17	5.82	2.48[f]
69	2-Cl	3-CH_3	6.22	5.98–6.46	6.88	3.11[d]
70	2-Cl	3-OCH_3	7.28	7.10–7.47	6.17	2.81[f]
71	2-Cl	4-F	6.41	6.25–6.56	6.15	2.87[d]
72	2-Cl	4-Cl	6.94	6.76–7.13	6.85	3.51[d]
73	2-Cl	4-Br	7.47	7.34–7.61	7.11	3.73[f]
74	2-Cl	4-I	8.12	7.93–8.31	7.68	3.96[f]
75	2-Cl	4-CF_3	8.00	7.79–8.21	6.91	3.68[f]
76	2-Cl	4-NO_2	5.46	5.31–5.61	5.81	2.78[f]
77	2-Cl	4-CN	6.22	6.13–6.33	6.61	2.44[f]
78	2-Cl	4-CH_3	7.73	7.52–7.83	7.26	3.15[d]
79	2-Cl	4-Et	8.24	8.09–8.38	7.76	3.59[f]
80	2-Cl	4-*n*-Pr	8.04	7.77–8.31	7.73	4.06[f]
81	2-Cl	4-*i*-Pr	7.61	7.40–7.82	8.16	4.11[f]
82	2-Cl	4-Ph	<4.00	—	7.24	4.49[f]
83	2-Cl	4-OCH_3	7.29	7.08–7.50	7.46	2.82[f]
84	2-Cl	4-SO_2CH_3	5.89	5.75–6.02	5.82	1.46[g]
85	2-Cl	4-$COCH_3$	6.98	6.84–7.11	6.93	2.42[g]
86	2-Cl	2,3-Cl_2	8.03	7.91–8.15	6.70	3.75[f]
87	2-Cl	2,3-$(CH_3)_2$	7.70	7.55–7.86	6.88	3.40[f]
88	2-Cl	2-CH_3-3-OCH_3	7.81	7.63–7.98	7.57	3.46[h]
89	2-Cl	2,4-Cl_2	6.65	6.44–6.85	6.67	3.71[f]
90	2-Cl	2,4-$(CH_3)_2$	6.79	6.60–6.97	7.35	3.38[f]
91	2-Cl	2,5-Cl_2	5.69	5.39–5.99	6.07	3.75[f]
92	2-Cl	2,5-$(CH_3)_2$	5.79	5.52–6.05	6.22	3.40[f]
93	2-Cl	2,6-F_2	7.53	7.41–7.66	6.41	2.35[f]
94	2-Cl	2-F-6-Cl	6.77	6.55–6.99	5.96	2.67[f]
95	2-Cl	2,6-Cl_2	5.17	5.00–5.35	5.78	3.03[f]
96	2-Cl	3,4-Cl_2	6.34	6.12–6.57	6.32	4.25[f]
97	2-Cl	3,4-$(CH_3)_2$	7.06	6.82–7.31	7.59	3.65[f]
98	2-Cl	3,5-Cl_2	6.42	6.09–6.75	6.11	4.29[f]
99	2-Cl	3,5-$(CH_3)_2$	5.07	4.82–5.32	6.19	3.67[f]
100	2-Cl	3,5-(O-*n*-Bu)$_2$	<4.00	—	6.04	5.63[f]
101	3,5-$(CH_3)_2$	2-CH_3	6.99	6.72–7.26	6.86	3.98[h]
102	3,5-$(CH_3)_2$	3-CH_3	7.55	7.35–7.75	7.29	3.98[h]
103	3,5-$(CH_3)_2$	3-OH	6.47	6.29–6.65	6.83	3.34[h]
104	3,5-$(CH_3)_2$	3-OCH_3	7.18	6.99–7.38	6.86	3.75[h]
105	3,5-$(CH_3)_2$	3-OEt	6.32	6.00–6.64	6.60	4.28[h]
106	3,5-$(CH_3)_2$	4-CH_3	7.92	7.75–8.10	8.09	3.95[f]
107[i]	3,5-$(CH_3)_2$	4-Et	8.91	8.70–9.12	8.40	4.39[f]
108	3,5-$(CH_3)_2$	4-*n*-Pr	7.88	8.04–8.73	8.38	4.86[f]
109	3,5-$(CH_3)_2$	4-*i*-Pr	8.87	8.66–9.08	8.92	4.91[f]
110	3,5-$(CH_3)_2$	4-*n*-Bu	6.75	6.56–6.95	8.05	5.39[j]
111	3,5-$(CH_3)_2$	4-*t*-Bu	8.61	8.43–8.78	8.93	5.31
112	3,5-$(CH_3)_2$	4-*n*-Pentyl	7.29	7.20–7.39	8.12	5.92[j]
113	3,5-$(CH_3)_2$	4-Cl	7.72	7.42–8.01	7.53	4.31[d]
114	3,5-$(CH_3)_2$	4-CF_3	8.43	8.21–8.65	7.58	4.66
115	3,5-$(CH_3)_2$	2,3-$(CH_3)_2$	8.62	8.45–8.79	7.83	4.43[h]
116	3,5-$(CH_3)_2$	2-CH_3-3-OH	6.89	6.70–7.09	7.10	3.84[h]
117[k]	3,5-$(CH_3)_2$	2-CH_3-3-OCH_3	8.22	8.05–8.39	8.03	3.93[g]
118	3,5-$(CH_3)_2$	2-CH_3-3-OEt	7.28	7.11–7.45	8.24	4.78[h]
119	3,5-$(CH_3)_2$	2,3,4-F_3	7.26	7.06–7.47	7.25	3.64
120	3,5-$(CH_3)_2$	2,4,5-F_3	7.31	7.16–7.47	7.01	3.71
121	3,5-Cl_2	4-CH_3	8.01	7.80–8.22	7.79	4.81[f]
122	3,5-Cl_2	4-Cl	7.16	6.81–7.51	7.10	5.17[f]
123	3,5-Br_2	2-CH_3	6.88	6.57–7.18	6.14	4.93

Table 1 (*continued*)

Compound	A-ring	B-ring	Activity (pEC_{50}, M)			Log P[b]
			Observed		Calculated[a]	
			pEC_{50}	95% CI	pEC_{50}	
124	3,5-Br_2	4-CH_3	7.68	7.42–7.94	7.99	5.07[f]
125	3,5-Br_2	4-Et	8.04	7.87–8.21	8.25	5.51[f]
126	3,5-Br_2	4-NO_2	6.72	6.54–6.91	6.62	4.38
127	2-CH_3	2-CH_3	6.55	6.26–6.85	6.42	3.48
128	4-Cl	4-Cl	6.39	6.17–6.62	6.42	4.13
129	4-Cl	4-CH_3	7.38	7.14–7.62	7.19	3.86
130	4-Et	4-Et	6.64	6.46–6.82	6.95	4.54
131	2,6-F_2	4-Cl	7.08	6.75–7.42	6.41	3.00
132	H	4-Et	8.31	8.12–8.49	7.79	3.51[j]
133[l]	H	4-Cl	7.06	6.88–7.23	6.89	3.37[g]

[a] Calculated by Eq. 2b.
[b] Unless noted, values were calculated for this work using CLOGP (BioByte Corp., Claremont, CA, USA).
[c] RH-5849.
[d] Experimentally measured by Oikawa et al.[42,43]
[e] Oikawa et al.[43]
[f] Oikawa et al.[42]
[g] Nakagawa et al.[54]
[h] Nakagawa et al.[21]
[i] Tebufenozide (RH-5992).
[j] Nakagawa et al.[18]
[k] Methoxyfenozide.
[l] Halofenozide.

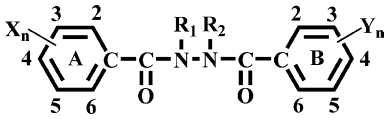

Figure 1. General template of dibenzoylhydrazines examined in this study. The A-ring and B-ring nomenclature are used throughout the work to describe the position of the relative CoMFA fields. The numbers on the aromatic rings refer to the positions of the different substituents (X and Y) listed in Tables 1–3. R_1 and R_2 refer to substitutions on the nitrogen atoms as listed in Tables 1–3. The atoms used for the CoMFA alignment are shown in the bridging backbone between the A- and B-ring, and consist of C–C–N–N–C–C.

than **107**. Replacement of the *tert*-butyl group with a cyclohexyl (**165**) as well as a CH_2-cyclohexyl (**166**) was unfavored. Substitution of both *N* atoms (**167**–**170**) resulted in complete loss of activity, most likely due to blockage of hydrogen bond formation with amino acid residues in the active site.[34,36] Replacement of the ketone alpha to the A-ring with a methylene moiety resulted in a reduction in the compound's potency as shown by **171** and **172**.

2.2. Three-dimensional QSAR with CoMFA

We performed CoMFA analyses for all the dibenzoylhydrazines in Table 1 (**1**–**133**), but excluded compounds that did not exhibit any biological activity (**10**, **12**, **13**, **31**, **32**, **82**, and **100**). Earlier studies had shown that the hydrophobic parameter ($\log P$) was important for describing the inhibitory activity of these compounds and it was therefore used in the development of the initial equations[37]

$$\begin{aligned} pEC_{50} &= 0.980\log P - 0.116(\log P)^2 \\ &\quad + [\text{CoMFA terms}] + 4.755, \\ n &= 126, \quad s = 0.457, \quad r^2 = 0.815, \quad F_{6,119} = 87.445 \\ (q^2 &= 0.506,\ S_{CV} = 0.747,\ m = 6); \\ &\text{Electrostatic } 32.5\%;\ \text{Steric } 47.0\%;\ \text{logP=}10.9\%; \\ (\log P)^2 &= 9.5\%\ \log P_{opt} = 4.22. \end{aligned} \tag{1a}$$

The resulting Eq. 1a provided an acceptable description of the biological observations; however, we found that removal of the hydrophobic parameter $\log P$ slightly improved the conventional correlation.

$$\begin{aligned} pEC_{50} &= [\text{CoMFA terms}] + 6.437, \\ n &= 126, \quad s = 0.436, \quad r^2 = 0.831, \quad F_{6,119} = 97.870 \\ (q^2 &= 0.479,\ S_{CV} = 0.768,\ m = 6); \\ &\text{Electrostatic } 44.0\%;\ \text{Steric } 56.0\% \end{aligned} \tag{1b}$$

We then attempted to formulate a CoMFA equation for all the active compounds ($n = 158$) examined in this study (**1**–**172**), shown with their structure and biological potency in Tables 1–3. The initial equation was again generated using $\log P$ terms and the resulting Eq. 2a is shown below.

$$\begin{aligned} pEC_{50} &= 1.312\log P - 0.155(\log P)^2 \\ &\quad + [\text{CoMFA terms}] + 1.188, \\ n &= 158, \quad s = 0.591, \quad r^2 = 0.701, \quad F_{4,153} = 89.473 \\ (q^2 &= 0.490,\ S_{CV} = 0.772,\ m = 4); \\ &\text{Electrostatic } 27.6\%;\ \text{Steric } 38.7\%; \\ &\log P = 17.8\%;\ (\log P)^2 = 15.9\%,\ \log P_{opt} = 4.23. \end{aligned} \tag{2a}$$

Table 2. Activity of *tert*-butyl-containing diacylhydrazines

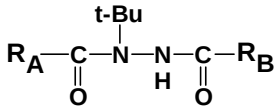

Compound	R_A	R_B	Activity (pEC_{50}, M)			Log P[b]
			Observed		Calculated[a]	
			pEC_{50}	95% CI	pEC_{50}	
134	Cyclohexyl	Ph	4.33	4.06–4.60	4.45	2.61
135	*n*-Hexyl (C6)	Ph	5.14	4.85–5.43	4.54	3.22
136	*n*-Pentyl (C5)	Ph(3,5-$(CH_3)_2$)	5.06	4.64–5.48	4.71	3.69
137	*i*-Pentyl (C5)	Ph(3,5-$(CH_3)_2$)	4.84	4.38–5.29	4.77	3.56
138	*i*-Hexyl (C6)	Ph(3,5-$(CH_3)_2$)	<4.00	—	4.41	4.09
139	*n*-Heptyl (C7)	Ph(3,5-$(CH_3)_2$)	5.19	4.86–5.51	4.54	4.75
140	*i*-Pr (C3)	Ph(4-Et)	4.26	3.92–4.60	5.16	2.44
141	*n*-Pentyl (C5)	Ph(4-Et)	5.55	5.13–5.96	6.00	3.72
142	*i*-Pentyl (C5)	Ph(4-Et)	6.08	5.79–6.38	6.17	3.59
143	*n*-Hexyl (C6)	Ph(4-Et)	4.93	4.18–5.67	5.43	4.25
144	α-Naphthyl	Ph(4-Et)	7.88	7.68–8.07	7.51	4.68
145	3-Cyclohexene	Ph(4-Et)	6.00	5.83–6.16	6.80	3.15
146	Cyclohexyl	Ph(4-Et)	5.03	4.75–5.30	5.46	3.63
147	Ph(2-Cl)	*n*-Hexyl (C6)	6.13	5.81–6.45	6.30	3.50
148	Ph(3,5-$(CH_3)_2$)	*n*-Butyl (C4)	5.73	5.47–5.99	6.45	3.16
149	Ph(3,5-$(CH_3)_2$)	*n*-Pentyl (C5)	7.10	6.94–7.26	6.93	3.69
150	Ph(3,5-$(CH_3)_2$)	*i*-Pentyl (C5)	7.04	6.90–7.17	6.88	3.56
151	Ph(3,5-$(CH_3)_2$)	*n*-Hexyl (C6)	7.28	7.04–7.52	7.22	4.22
152	Ph(3,5-$(CH_3)_2$)	*i*-Hexyl (C6)	7.36	7.14–7.57	7.22	4.09
153	Ph(3,5-$(CH_3)_2$)	*n*-Heptyl (C7)	7.01	6.80–7.22	6.73	4.75
154	Ph(3,5-$(CH_3)_2$)	*n*-Nonyl (C9)	5.81	5.43–6.18	6.45	5.80

[a] Values were calculated using Eq. 2b.
[b] Calculated by CLOGP (MacLogP ver. 4.0).

However, we again found that exclusion of the hydrophobic parameter slightly increased the quality of the correlation as shown in Eq. 2b.

$$pEC_{50} = [\text{CoMFA terms}] + 4.041,$$
$$n = 158, \quad s = 0.554, \quad r^2 = 0.737, \quad F_{4,153} = 107.199$$
$$(q^2 = 0.447,\ S_{CV} = 0.781,\ m = 4);$$
$$\text{Electrostatic } 42.1\%; \text{Steric } 57.9\%. \qquad (2b)$$

The superposition of the compounds used in Eq. 2b is displayed in Figure 2 and the atoms chosen for the alignment are shown in Figure 1. In general, the steric and electronic contours were nearly identical for the inclusion or exclusion of log P parameters and the resulting CoMFA fields were relatively uncomplicated. Therefore, the displayed results are only for the exclusion of log P (Eq. 2b). Figures 3 and 4 show the respective contour maps for the steric and electrostatic fields with tebufenozide as the template molecule. Important observations include a large region of unfavorable steric activity surrounding the edge of the 4-position of the A-ring and a sterically favorable region surrounding the ethyl substituent in the 4-position of the B-ring. The 3- and 5-positions of the B-ring have sterically unfavorable fields surrounding them. The electrostatic fields show a positive field around the 2- and 3-positions of the A-ring, with negative fields over the oxygen atoms of the bridge and a positive field over the NH moiety. Additional negative fields were observed around the 2-, 3-, and 6-positions of the B-ring, with positive fields around the 5-position. A large positive field surrounds the 2-, 3-, and 4-positions of the B-ring.

A few small differences were observed in the CoMFA fields following the inclusion of log P terms (Eqs. 2a vs 2b; data not shown). The electrostatic potential displayed key differences surrounding the 4-position of the A-ring, with a much larger positive field observed with the inclusion of log P values. Significant reductions in both negative and positive electrostatic fields were observed surrounding the 4-position of the B-ring. The greatest effect was the lack of large negative and positive fields at the end of the ethyl substituent on the 4-position of the B-ring in the absence of log P. The steric fields, on the other hand, evidenced very few differences with a slight reduction in favorable steric activity surrounding the ethyl substituent in the 4-position of the B-ring in the absence of log P. The hydrophobic effects were further examined with a comparative molecular similarity index analysis (CoMSIA);[38] however, the resulting equation was inferior to the CoMFA analysis (data not shown). Eq. 2b was subsequently chosen as the final equation to calculate the pEC_{50} values shown in Tables 1–3. This equation was able to describe approximately 74% of the biological activity for 158 active compounds as shown in Figure 5.

Table 3. Activity of various N-substituted dibenzoylhydrazines and benzyl analogs

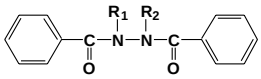

Compound	R_1	R_2	Activity (pEC_{50}, M)			Log P[b]
			Observed		Calculated[a]	
			pEC_{50}	95% CI	pEC_{50}	
155	CH_3	H	<4.00	—	6.11	1.25
156	Et	H	<4.00	—	6.11	1.77
157	*i*-Pr	H	5.24	5.07–5.42	5.86	2.08
158	*n*-Bu	H	5.15	4.78–5.53	5.60	2.83
159	*i*-Bu	H	5.54	5.37–5.71	5.66	2.70
160	*sec*-Bu	H	5.70	5.54–5.85	6.15	2.61
161	2-Methylbutyl	H	6.18	5.88–6.48	5.96	3.23
162	*tert*-Amyl	H	6.81	6.65–6.97	5.89	3.01
163	Ph	H	4.59	4.35–4.83	4.57	3.15
164	Ph(4-F)	H	4.89	4.72–6.05	4.58	3.30
165	Cyclohexyl	H	6.05	5.90–6.19	6.20	3.28
166	CH_2-Cyclohexyl	H	5.77	5.58–5.95	5.43	3.90
167	CH_3	CH_3	<4.00	—	5.84	2.74
168	*tert*-Bu	CH_3	<4.00	—	6.35	3.97
169	*tert*-Bu	*n*-Bu	<4.00	—	6.18	5.56
170	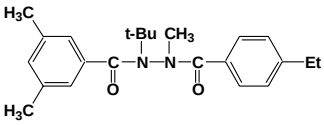		<4.00	—	8.52	6.00
171	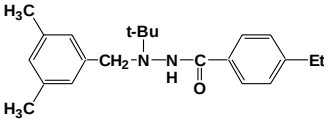		5.90	5.69–6.11	5.95	6.09
172	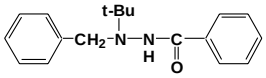		5.04	4.73–5.34	5.87	4.06

[a] Values were calculated using Eq. 2b.
[b] Calculated by CLOGP (MacLogP ver. 4.0).

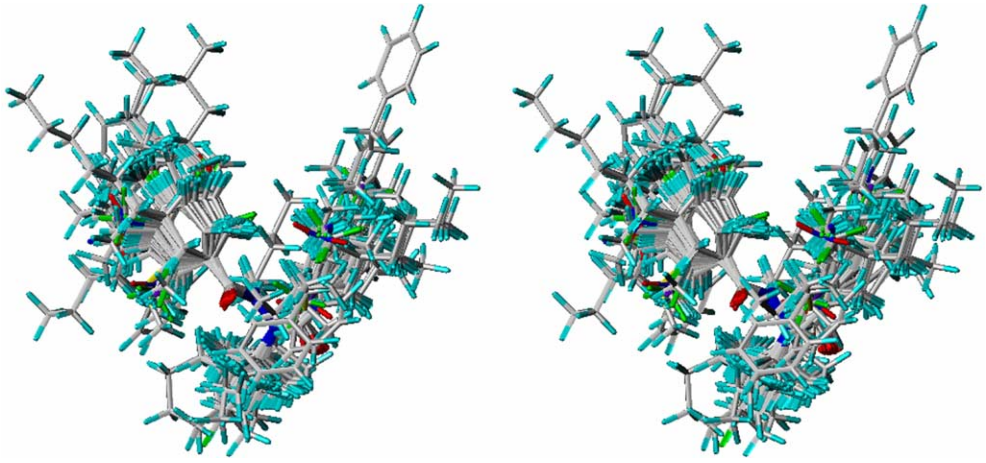

Figure 2. Stereoview of the superposition of all 172 compounds analyzed in this study.

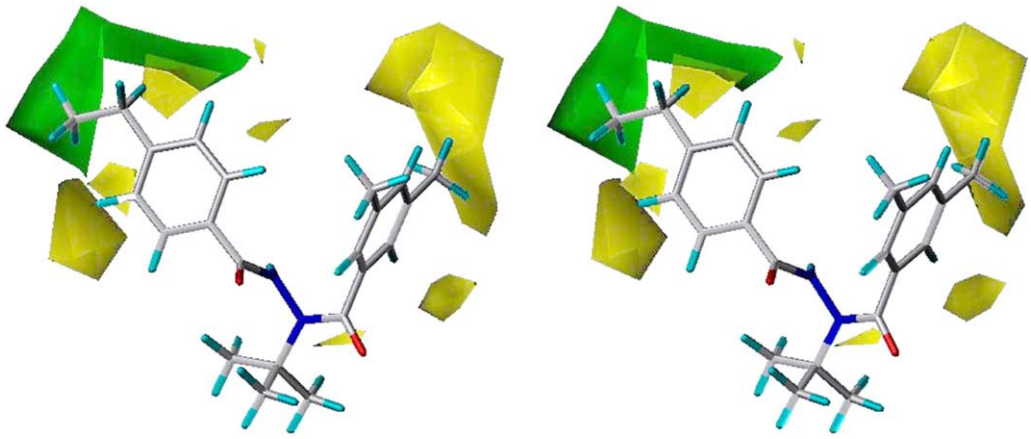

Figure 3. Stereoviews of the CoMFA fields generated with Eq. 2b (absence of log *P*) using tebufenozide (compound **107**) as the template. Contours are shown to surround regions where increased steric bulk increase (green) or decreases (yellow) the biological activity.

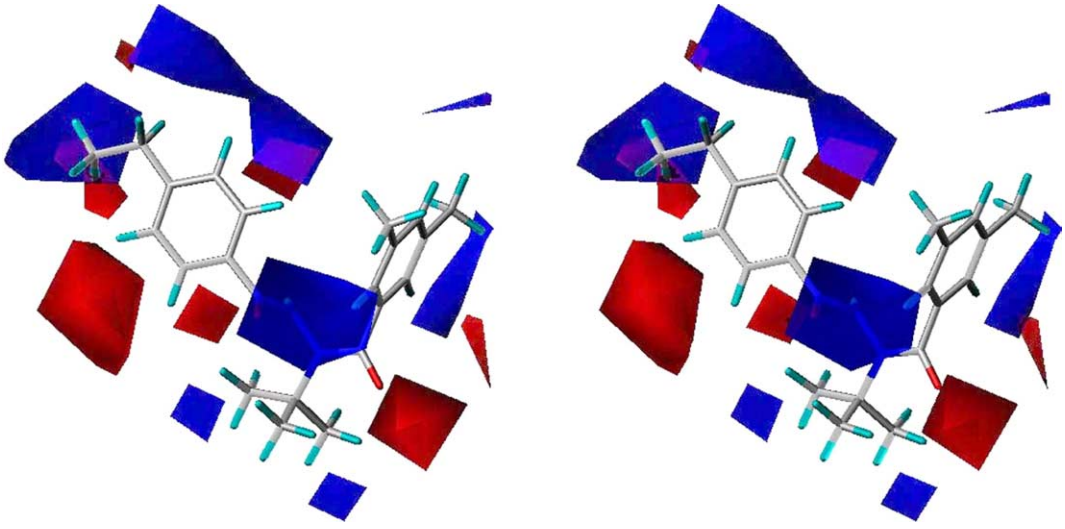

Figure 4. Stereoviews of the CoMFA fields generated with Eq. 3 (absence of log *P*) using tebufenozide (compound **107**) as the template. Contours are shown to surround regions where a positive (blue) or negative (red) electrostatic potential increases the biological activity.

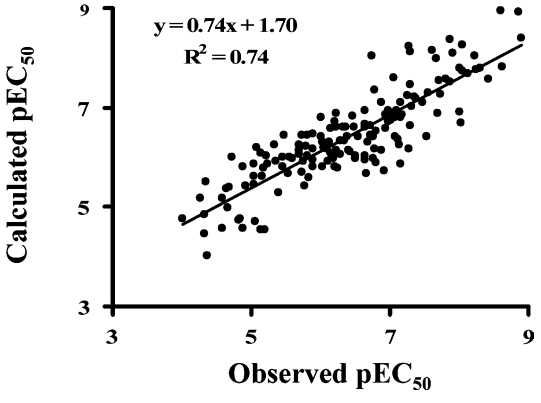

Figure 5. Linear correlation of predicted versus experimental pEC_{50} values for the 158 compounds used in Eq. 2b.

2.3. Ecdysone receptor modeling

Modeling studies were performed in order to further understand the physicochemical parameters that are important for ligand activity. A model of the *B. mori* EcR receptor binding pocket was generated based upon the *Heliothis virescens* structure previously published (Fig. 6).[34] The results of the CoMFA steric map were then superimposed over the surface of the EcR binding pocket to show the steric interactions (Fig. 7). The results show that the ligand (tebufenozide, **107**) fits tightly into the receptor, but that there is potential room for expansion (groups with increased steric bulk) in the upper left-hand portion of the receptor. The limits on steric bulk (yellow areas) correspond to the boundaries of the receptor, except for the *tert*-butyl group, where no field is visualized. This observation is probably due to the fact that the structural variety of the *N*-alkyl groups is limited and that no biological activity was observed for compounds containing small N-substituted groups such as CH_3 (**155**) or ethyl (**156**).

The modeling studies also showed that the orientation of tebufenozide in the binding pocket enables it to undergo both hydrophobic and hydrophilic interactions

```
Bm   331 PFRQITEMTI LTVQLIVEFA KGLPGFSKIS QSDQITLLKA SSSEVMMLRV ARRYDAASDS 390
Hv   335 PFRQITEMTI LTVQLIVEFS KGLPGFSKIS QSDQITLLKA CSSEVMMLRV ARRYDAATDS 394
Bt   223 RFRHITEITI LTVQLIVEFS KRLPGFDKLI REDQIALLKA CSSEVMMFRM ARRYDAETDS 282

Bm   391 VLFANNKAYT RDNYRQGGMA YVIEDLLHFC RCMFAMGMDN VHFALLTAIV IFSDRPGLEQ 450
Hv   395 VLFANNQAYT RDNYRKAGMA YVIEDLLHFC RCMYSMMMDN VHYALLTAIV IFSDRPGLEQ 454
Bt   283 ILFATNQPYT RESYTVAGMG DTVEDLLRFC RHMCAMKVDN AEYALLTAIV IFSERPSLSE 342

Bm   451 PSLVEEIQRY YLNTLRIYII NQNSASSRCA VIYGRILSVL TELRTLGTQN SNMCISLKLK 510
Hv   455 PSLVEEIQRY YLNTLRVYIL NQNSASPRSA VIFGKILGIL TEIRTLGMQN SNMCISLKLK 514
Bt   343 GWKVEKIQEI YIEALKAYVE NRR--KPYAT TIFAKLLSVL TELRTLGNMN SETCFSLKLK 402

Bm   511 NRKLPPFLEE IWDVA  525
Hv   515 NRKLPPFLEE IWDVA  529
Bt   403 NRKVPSFLEE IWDVV  416
```

Figure 6. Sequence alignment of ligand-binding domains between the *Bombyx mori*, *Heliothis virescens*, and *Bemisia tabaci* ecdysone receptors (EcR). The numbering of the first amino acid (P331) of BmEcR is the same as that reported by Kamimura et al.[51] and corresponds to P394 reported by Swevers et al.[35] The numbering of HvEcR and BtEcR is the same as that reported by Billas et al.[34] and Carmichael et al.,[39] respectively. Regions in yellow are highlighted to show areas of sequence conservation. Residues in red are located within 3 Å from the ligand.

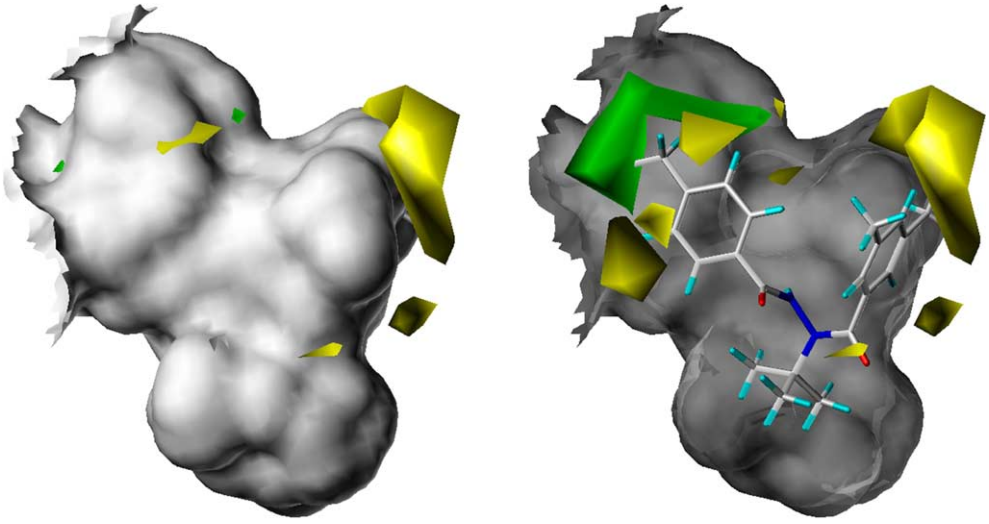

Figure 7. Surface of the EcR binding pocket overlaid with the CoMFA steric fields. Tebufenozide (compound **107**) is used as the template and contours are shown to surround regions where increased steric bulk increases (green) or decreases (yellow) the activity.

that most likely support its binding geometry. These interactions were expected based upon previously published work with the EcR receptor.[34,39] However, it was interesting to compare our model with published structures. Results agree with the current theory of binding of diacylhydrazine, which involves a series of hydrophobic and hydrophilic interactions. The *tert*-butyl group is surrounded by a number of hydrophobic amino acids including M409, M503, L507, and L514 as shown in Figure 8. These groups surround the pocket containing the *tert*-butyl and are most likely involved in the need for a large steric moiety in this portion of the molecule. The amino acids T339, Y404, and N500 are in a position to form hydrogen bonds with the bridge of the diacylhydrazine moiety (Fig. 9). The hydrogen-bonding groups of all of these amino acids (the NH_2 and OH moieties) are within 2.0–2.5 Å of the corresponding groups of the diacylhydrazine moiety.

3. Discussion

3.1. Molting hormonal activity

Non-steroidal ecdysone agonists such as the dibenzoylhydrazines represent an important class of insect control agents. Their target selectivity makes them a useful tool in controlling crop pests. It is therefore important that the mechanism of agonist binding be well understood to increase our ability to construct new potent and selective agonists. This project was designed to examine the compound substructures that are essential for biological activity and to evaluate the utility of a new high-throughput screening system for agonist activity. These results are described by Eq. 2b, which shows that we were able to obtain a reasonable model for the array of compounds examined in this study without excluding any active compounds.

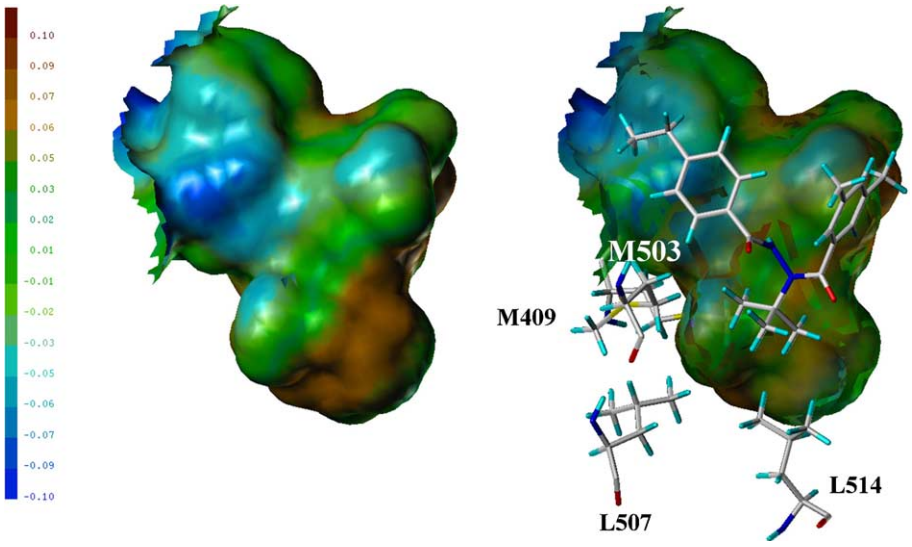

Figure 8. Hydrophobic surface gradient. The solvent accessible surface of the optimized structure was expressed using the MOLCAD module of SYBYL using the Fast Conolley algorithm. There are no physical units for the value (unlike experimental log *P*); however, the color gradient of the hydrophobicity of the receptor surface ranges from blue (highest hydrophilic area) to brown (highest lipophilic area). The color scheme is best interpreted by associating blue with water and brown with oil or fat. M = methionine and L = leucine.

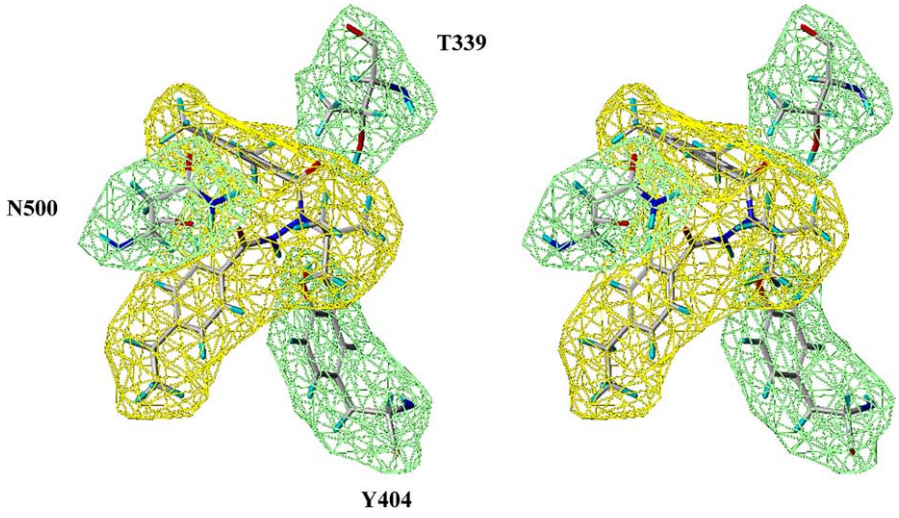

Figure 9. Hydrophilic amino acids that are in a position to form hydrogen bonds with the agonist (tebufenozide, compound **107**). The hydrogen-bonding groups of the amino acids (NH_2 or OH moiety) are in a position to form hydrogen bonds (2.0–2.5 Å) with the diacylhydrazine moiety. The green and yellow maps indicate the solvent accessible surface areas of the amino acids of the receptor and the ligand, respectively. T = threonine, Y = tyrosine, and N = asparagine.

A necessary exercise was to determine the extent to which data collected with this new *B. mori* assay could be compared to existing data from other assay systems. We therefore examined the relationship between pEC_{50} values measured with the *B. mori* system and the binding activity of various dibenzoylhydrazines using *Spodoptera frugiperda*-derived cells (Sf-9)[40] and molting hormonal activity in an in vitro system using integument parts of *C. suppressalis*[16,17] as shown in Eqs. 3 and 4:

$$\begin{aligned} pEC_{50}\ (B.\ mori) &= 0.886(\pm 0.193)pIC_{50}(Sf9) \\ &\quad + 0.809(\pm 1.383), \qquad (3) \\ n = 47, \quad s = 0.468, \quad r^2 &= 0.809, \end{aligned}$$

$$\begin{aligned} pEC_{50}\ (B.\ mori) &= 0.931(\pm 0.122)pIC_{50}(Chilo) \\ &\quad + 0.325(\pm 0.821), \qquad (4) \\ n = 61, \quad s = 0.497, \quad r^2 &= 0.893. \end{aligned}$$

Forty-seven compounds were used to derive Eq. 3: **1**, **3**, **11**, **16**, **47**, **57**, **58**, **69–81**, **83–85**, **87**, **88**, **93**, **101–105**, **107**, **110**, **115–118**, **132**, **133**, and **147–154**, and 61 compounds were used in Eq. 4: **1**, **3**, **7**, **8**, **11**, **15**, **16**, **19–22**, **24**, **26**, **28–30**, **33**, **52–54**, **56**, **58**, **60**, **63**, **65–67**, **69**, **72–78**, **83**, **106–110**, **112**, **117**, **132–134**, **141–146**, **148–154**, and **171**, **172**. The observed activity using the *B. mori* reporter gene assay correlated fairly

well with the activity measured using other assay systems. As these assays all employ *Lepidoptera* insects, a high degree of correlation was expected. However, the correlation data are useful in that they enable us to directly compare results measured with the different assay systems.

Although the three assay systems are specific to lepidopteran insects (*S. frugiperda*, *C. suppressalis*, and *B. mori*), clear differences exist with respect to the assessment of molting hormone activity. In the Sf-9 cell-based assay, binding activity is measured against protein extracts derived from the cellular nuclei. Therefore, no inhibition is expected that is related to the necessity of the compound to transverse cellular membranes. Moreover, simple binding does not necessarily implicate that the bound compound is capable of activating transcription. The *B. mori*-based cell assay and *C. suppressalis*-based integument assay therefore more accurately (although not perfectly) reflect in vivo conditions. Differences between the *B. mori*- and *C. suppressalis*-based systems probably relate to penetration differences between the two systems (e.g., the existence of a basal membrane barrier in the integument assay as opposed to cells in tissue culture that do not have a basal membrane). The duration of the required response to detect an effect can also differ between the two assays. In the *B. mori*-based system, a direct response to ecdysone is detected, while the response in the integument system is achieved only after the completion of the ecdysone regulatory cascade that involves different layers of primary and secondary response genes as well as feedback mechanisms that occur over a period of several days. Differences between the assay construction and physical parameters could therefore explain the species-specific variations observed for compound activity. Alternatively, the differences may be due to variation in the structure of the individual ecdysone receptors. To distinguish between the possibilities, differently constructed assays should be performed for the same species or assays of the same set-up should be carried out for different species. For instance, the molting hormonal activity in *B. mori* can be compared by (1) competition with [^{3}H]PonA for binding to nuclear extracts; (2) reporter gene activation in cell lines; and (3) induction of molting in larval integument in vitro. A more attractive possibility would be the generation of high-throughput systems based on the cell lines of other lepidopteran species, in a similar fashion as carried out for *B. mori*.

3.2. Three-dimensional QSAR with CoMFA

The CoMFA analyses provided a number of insights into the mechanism of agonist binding. Of particular interest was the observation that $\log P$ effects were not important for describing biological activity. Log P is the octanol–water partition coefficient and is defined as the ratio of the concentration of a chemical in octanol and in water at equilibrium (at a specified temperature). This partition coefficient has been adopted as the standard measure of lipophilicity, which governs the mass flux of a molecule in a physical or biological system. Solubility in a lipophilic organic phase increases with the lipophilicity of a molecule. Tables 1–3 list the predicted pEC_{50} values calculated using Eq. 2b (exclusion of $\log P$). We also performed the calculation with Eq. 2a (CoMFA views not shown) and found that it was generally inferior to Eq. 2b at predicting the observed biological activity. For example, the three commercial compounds examined in this study (tebufenozide **107**, methoxyfenozide **117**, and halofenozide **133**) resulted in the following: for **107** the observed pEC_{50} was 8.91 and predicted with Eq. 2a was 8.14 versus 8.40 with Eq. 2b, for **117**, observed pEC_{50} was 8.22 and predicted with Eq. 2a was 7.94 versus 8.03 with Eq. 2b, and for **133** the observed pEC_{50} was 7.06 and predicted with Eq. 2a was 6.75 versus 6.98 with Eq. 2b. These results were typical in that Eq. 2a consistently underpredicted the pEC_{50} value.

Earlier work with these compounds in a different assay system had shown that $\log P$ was important for describing activity. We performed similar 3-D QSAR CoMFA studies using data obtained from the examination of the ability of dibenzoylhydrazine derivatives to displace [^{3}H]PonA binding to nuclear extracts of Sf-9 cells.[37] This equation consisted of 50 compounds including 46 compounds, **1**, **3**, **11**, **16**, **47**, **57**, **58**, **69–81**, **83–85**, **87**, **88**, **93**, **101–105**, **107**, **110**, **115–118**, **132**, **133**, and **148–154**, from the current study. Since four compounds did not overlap between the present and previous study, those compounds were omitted and the remaining compounds were reanalyzed to derive Eq. 5a as the best descriptor of biological activity[37]

$$\begin{aligned} pIC_{50} &= 1.772\log P - 0.228(\log P)^2 + [\text{CoMFA terms}] \\ &\quad + 2.913, \qquad (5a) \\ n &= 46, \quad s = 0.269, \quad r^2 = 0.868, \quad F_{5,40} = 52.636, \\ (q^2 &= 0.486,\ S_{CV} = 0.530,\ m = 5); \\ &\text{Electronic } 16.7\%,\ \text{Steric } 29.8\%,\ \log P = 27.8\%, \\ (\log P)^2 &= 25.8\%,\ \log P_{opt} = 3.89. \end{aligned}$$

However, a reanalysis of the same data shows that removal of the $\log P$ terms provides a significant equation, with increased r^2 and F values, but using an additional component ($m = 6$ for Eq. 5b vs $m = 5$ for Eq. 5a) and giving poor q^2 and S_{CV} values in the cross-validation analysis

$$\begin{aligned} pIC_{50} &= [\text{CoMFA terms}] + 5.713, \qquad (5b) \\ n &= 46, \quad s = 0.228, \quad r^2 = 0.907, \quad F_{6,39} = 63.660 \\ (q^2 &= 0.334,\ S_{CV} = 0.611,\ m = 6); \\ &\text{Electronic } 37.3\% \text{ Steric } 62.7\%. \end{aligned}$$

These observations are interesting in that the CoMFA fields clearly show that there are distinct areas of favorable and unfavorable steric fields. However, these effects do not appear to be correlated explicitly with hydrophobicity. Furthermore, given the similarities between Eqs. 5a and 5b (and Eqs. 2a and 2b), it would seem that in general hydrophobicity parameters are not necessary for describing the activity of these dibenzoylhydrazine analogs. Another possible explanation lies in the inher-

ent nature of the CoMFA analysis. It is difficult to separate $\log P$ effects from the electrostatic potential and steric fields generated by the CoMFA model. The nature of the analysis for especially the steric fields contains a hydrophobic component, essentially inherently accounting for $\log P$ effects. It is therefore not surprising that direct inclusion of the $\log P$ term does not have a significant impact upon the generated CoMFA equations. However, other CoMFA studies have reported that the inclusion of $\log P$ terms can dramatically affect the outcome of analyses.[41]

Interestingly, we previously reported that molecular hydrophobicity was an important parameter in classical QSAR for the activity against *Lepidoptera*.[17,42,43] In light of the above discussion, these results are not necessarily at odds as it first appears. Log P is undoubtedly important in the biological activity of these compounds, as evidenced by numerous structure–activity relationships. However, in the creation of CoMFA models, hydrophobic effects are not separated from the rest of the model generation. It is possible that if the hydrophobic contribution is small compared with other steric and electrostatic effects, then the hydrophobic terms will be reflected in the steric and electrostatic terms. However, attempts to further break down the fields into their individual components with the CoMSIA analysis were not useful. Limited improvement in CoMFA model performance upon the addition of hydrophobicity parameters (such as $\log P$) has been previously reported.[44] To further explore these observations, we conducted a classical QSAR analysis of a similar set of compounds. To simplify the analysis, we focused on only mono-substituted compounds. There were 29 compounds containing mono-substitution on the A-ring, which gave the following equation:

$$\mathrm{pEC}_{50} = -0.483(\pm 0.127)B_5^{\mathrm{para}} + 0.939(\pm 0.229)\sigma + 6.018(\pm 0.157), \quad (6a)$$

$$n = 29, \quad s = 0.321, \quad r^2 = 0.861, \quad F_{2,26} = 81.166.$$

In Eq. 6a, B_5^{para} is the steric parameter defined by Verloop and σ is Hammett's electronic parameter.[45] The values in parentheses are 95% confidence intervals of the regression coefficients. Similar studies performed with the 34 mono-substituted compounds on the B-ring provided a poorer correlation.

$$\mathrm{pEC}_{50} = -1.160(\pm 0.716)\sigma - 0851(\pm 0.326)B_5^{\mathrm{ortho}} - 0.424(\pm 0.417)B_5^{\mathrm{meta}} + 7.409(\pm 0.340) \quad (6b)$$

$$n = 34, \quad s = 0.622, \quad r^2 = 0.551, \quad F_{3,30} = 12.284.$$

Eq. 6b shows that electron-donating groups are favorable (as opposed to the A-ring) and that the steric effect of *para*-substituents is insignificant, although *ortho*- and *meta*-substituents are sterically unfavorable. These results are consistent with the CoMFA fields shown in Figures 3 and 4. While the size and statistical strength of Eqs. 6a and 6b are limited, the equations do suggest that $\log P$ terms are not necessary for describing activity. These results combined with the CoMFA studies in this work suggest that the biological activity of these dibenzoylhydrazines can be adequately described without the use of $\log P$ parameters. Further work could examine this premise by performing a more thorough classical QSAR analysis that included multiple substitutions on the A- and B-rings.

None of the new dibenzoylhydrazines tested exhibited biological potency greater than that of tebufenozide (**107**). This observation is displayed in the CoMFA fields in that any substitution on the A-ring was sterically unfavorable. The electronic fields did not show any significant areas of increased activity around the A-ring in the absence of $\log P$. However, with the inclusion of $\log P$ a field of positive electrostatic potential was observed around the A-ring (data not shown). Although this type of observation has been shown before to be associated with positive interactions of hydrogen atoms, it nevertheless does suggest one potential novel area of chemistry to be explored in future studies. For instance, the incorporation of particular electron deficient moieties could lead to improvements in activity. However, given the requirement for the compound to cross-cellular membranes, the addition of charged moieties is not advised.

The electrostatic fields surrounding the bridging backbone (area between the A- and B-ring) displayed fields similar to those previously reported.[37] The large positive electrostatic fields display the requirement for at least one hydrogen-substituted nitrogen atom on the hydrazine bridge for biological activity as evidenced by the lack of activity for compounds **167**–**170**. The negative field over the oxygen atom of the ketone displays the importance of this atom in activity. Substitution of this ketone with a methylene group resulted in a 3 orders of magnitude reduction in potency (**171** vs **107**). Also the 3-position of the B-ring displayed a region where negative electrostatic potential is favorable for activity. This activity was shown by compounds containing electron-rich groups in this position such as **70**, **88**, and **103**–**105**, **116**–**118**, which all contain an oxygen-substituted group in the *meta* position. It therefore may be useful to prepare a molecule that incorporates an electron-rich group in the 3-position in addition to the key ethyl moiety in the 4-position.

Other areas for potential improvements in agonist activity include the substituent on the hydrazine moiety. It is vital to have an N-substituted sterically bulky group (e.g., *tert*-butyl) as well as an unsubstituted (free hydrogen) group for compound activity. However, the optimal size of the bulky group is still in question. Comparison of compound **162** with **1** shows that the *tert*-amyl substitution slightly increases agonist potency. However, replacement with a cyclohexyl (**165**) reduces potency. The differences in the Connolly-solvent excluded volumes between a *tert*-amyl group and cyclohexyl group are small (94.7 and 100.8 Å^3, respectively) relative to that of a *tert*-butyl group (77.0 Å^3). An examination of Fig. 7 shows that there appears to be more room in the binding pocket surrounding the *tert*-butyl group. In addition, Figure 8 shows that this portion of the binding pocket is very lipophilic. It is very possible that a *tert*-amyl group is the optimal molecular volume;

however, the remaining structure of **162** has not been optimized and lacks the 3,5-dimethyl substitution on ring A as well as the *para*-ethyl on ring B. This compound would be a logical choice for further synthesis efforts. The other area of agonist structure that should be examined includes the permissible size of the A- and B-rings. Figure 3 shows that there is a favorable area of steric bulk surrounding the *para* position (site of the *para*-ethyl group) on the B-ring. This area could be explored by substitution with a bulky group such as an adamantyl moiety. The CoMFA fields suggest that the area surrounding the A-ring is at a steric maximum and further steric bulk in this area will not be favorable. These different areas can be targeted in an attempt to increase the potency and/or specificity of ecdysone agonists.

3.3. Ecdysone receptor modeling

The modeling studies supported the results of the CoMFA analyses. Of particular interest was the observation that the three key hydrophilic amino acid residues appeared to be serving the same role in the *B. mori* EcR as those observed in the lepidopteran *H. virescens* and hemipteran *Bemisia tabaci* EcRs.[34,39] In *B. mori*, the T339, Y404, and N500 triad appears to be in an equivalent position to form hydrogen bonds (2.0–2.5 Å) with the diacylhydrazine moiety (Fig. 9). The importance of these hydrogen-bonding interactions can be observed by examining compounds in which the key hydrogen-bonding moiety has been removed. In *B. mori*, the OH group of Y404 forms a hydrogen bond with the N–H moiety of the hydrazine and replacement of the hydrogen atom (**107**) with a methyl group (**170**) results in a complete loss of compound activity ($pEC_{50} < 4.00$). The *B. mori* T339 forms a hydrogen bond to the carbonyl moiety alpha to the A-ring. Replacement of the carbonyl with a methylene group results in a 3 orders of magnitude loss in activity (**107**, $pEC_{50} = 8.91$ to **171**, $pEC_{50} = 5.90$). Therefore, any further attempts at refining the structure–activity relationships of these compounds must ensure that these hydrogen-bonding moieties are not replaced.

4. Conclusion

We have shown that a cell-based reporter assay system using *B. mori* cells is useful for measuring dibenzoylhydrazine molting hormone activity in a high-throughput screening assay. 3-D QSAR analyses with CoMFA in conjunction with modeling of the *B. mori* EcR receptor show several key areas for agonist interaction with the binding pocket. These interactions can be possibly further optimized as discussed above. Analyses of the observed biological activity using CoMFA demonstrated that log *P* is not explicitly important for generating a significant equation. However, earlier results using classical QSAR had demonstrated that log *P* is an important parameter for describing biological activity. These divergent findings suggest that hydrophobic parameters are implicitly included within the CoMFA analysis and it is not necessary to explicitly include them in CoMFA analyses performed with dibenzoylhydrazines. Of particular importance is the high degree of correlation between QSAR analyses (both classical and 3-D) performed with this new *B. mori* system and those conducted with other screening systems (*Chilo* integument or Sf-9 cells). These results suggest that it is appropriate to compare the results, at least rank order potency, between different studies. This new assay system should greatly increase the speed and ease with which screening for novel ecdysone agonists can be performed.

5. Experimental

5.1. Bioassays

GFP fluorescence reporter gene assays were performed using the cell-based screening method of Swevers et al. and are briefly described here.[35] Fifty thousand cells of one of the Bm5/ERE.gfp clonal cell lines (permanently transformed with an ecdysone-responsive GFP reporter cassette L5Q or L6Q) were distributed in individual wells of a 96-well plate and treated with different concentrations of dibenzoylhydrazine compounds dissolved in 1 μl of dimethylsulfoxide (DMSO). Twenty-four hours after challenge, GFP fluorescence was quantified using a FLUOstar Galaxy Unit microplate fluorometer (BMG Lab Technologies, Offenburg, Germany) using a filter set with excitation filter 485 ± 10 nm and emission filter 530 ± 20 nm. In all measurements, background fluorescence was subtracted and values were expressed as percent of maximum fluorescence. Initially, a wide range of concentrations (10^{-5} to 10^{-11} with 10-fold differences between each concentration) was used to determine the approximate potency of the compounds. To determine more exact EC_{50} values, intermediary concentrations (2- to 3-fold differences) were also tested. EC_{50} values were calculated using the GraphPad Prism Program software (GraphPad Software, San Diego, CA) and were derived from at least three different series of measurements at concentrations that span the activation curve of each compound.

5.2. QSAR analyses

The Hansch–Fujita QSAR analysis was performed using QREG system ver.2.05.[46] Log *P* (where *P* is the partition coefficient in a 1-octanol–water system) values were taken from the literature[16,42,43] or calculated using the CLOGP program MacLogP Ver.4.0 (BioByte Corp., Claremont, CA, USA).[47] In all equations, *n* is the number of compounds used for the regression analyses, *s* is the standard deviation, *r* is the correlation coefficient, and the values in parentheses represent the 95% confidence intervals of the regression coefficient and the intercept. All CoMFA computations were performed with the molecular modeling software package Sybyl ver 6.91 (Tripos Co., St. Louis, MO, USA). The structures were generated by modifying the structure of RH-5849 (**1**), whose X-ray structure has been previously reported.[15] The geometry of all structures was fully optimized using PM3 and charges were calculated using AM1.

Compounds were automatically aligned using the Sybyl module Align Database and the common skeletal chain C–C–N–N–C–C shown in Figure 1 was used as a template. The molecules were superposed in a lattice space of $25.04 \times 28.65 \times 21.61$ Å ($X = -9.84$ to 15.20, $Y = -14.83$ to 13.82, and $Z = -9.93$ to 11.68). The superposition of all 172 compounds is shown in Figure 2. The CoMFA analyses were performed using the Sybyl QSAR module with a lattice spacing of 2 Å. The electrostatic and steric fields were estimated using a +1 charge and a sp^3 carbon, respectively. The electrostatic and steric potential energies at each lattice point were calculated using Coulombic and Lennard–Jones potential functions, respectively. Hydrophobic effects were evaluated using both $\log P$ and $(\log P)^2$ as lattice independent external descriptors. Correlation analyses were analyzed using partial least squares (PLS).[48] The number of latent variables in the set was initially selected using the leave-one-out method with the column filtering set at 2 kcal/mol. Conventional analyses were then performed using the optimum number of components, *m*. The CoMFA results are displayed using several statistical values: the leave-one-out cross-validated correlation coefficient, q^2, the cross-validated standard error, S_{cv}, the conventional correlation coefficient, *r*, and the standard deviation, *s*. The relative percentage contribution of each descriptor to the correlation equations is also shown. Results were visualized using contour maps that have connected lattice points that contain an equivalent coefficient level for each molecular field.

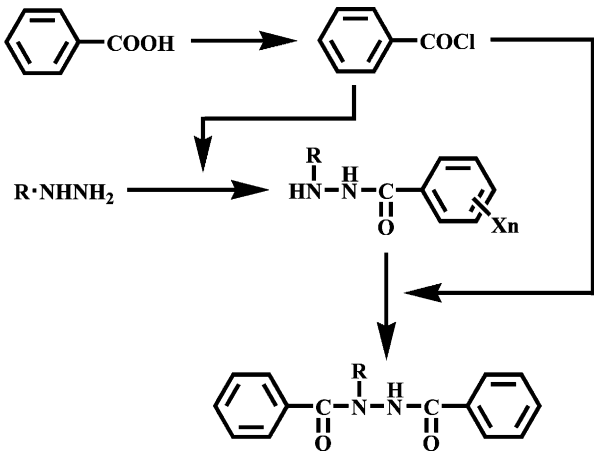

Scheme 1. Synthesis of *N-tert*-butyl-*N*,*N*′-dibenzoylhydrazines using *tert*-butylhydrazine and substituted benzoyl chloride as the starting materials.

5.3. Modeling

The homology modeling software PDFAMS (Protein Discovery Full Automatic Modeling System; In-Silico Sciences, Inc.; Tokyo, Japan), whose proto-type software FAMS was developed by Ogata and Umeyama,[49] was used to construct the ligand-binding region of *B. mori* EcR. In addition to the basic module PDFAMS pro, the optional module, PDFAMS-ligand is useful for proteins that are combined with ligands. The module was used to predict the protein structures in this study. These programs construct a tertiary structure of the target protein using the information from homologous proteins. The method consists of a database search, with the resulting structure minimized by the simulated annealing procedure. Processes such as searches for homologous proteins, alignment, construction of Cα-atoms, main-chain construction, and side-chain construction with the optimization of main-chain were performed automatically in an iterative fashion.

In the first step, primary sequences of BmEcR[50,51] obtained from the NCBI web site were aligned with homologous sequences in the FAMS database of PDFAMS. In this alignment, two homologous proteins were listed. The most homologous protein was 1R1K, a crystal structure of the ligand-binding domain of the heterodimer EcR–USP of the the lepidopteran *H. virescens* bound to steroidal ligand, PonA.[34] However, in this study, the alignment file was manually constructed using 1R20, HvEcR–USP with a DBH-type ligand BYI06830, as a reference protein. Although 1R20 was absent in the FAMS alignment database because of its sequence similarity to 1R1K (98%), the crystal structures showed that the ligand-binding pockets of 1R20 and 1R1K were only partially overlapped. Therefore, 1R20 was considered to be the best protein for the modeling of the BmEcR–DBH complex. In the second step, the three-dimensional structure of the ligand-binding domain of BmEcR was constructed from 1R20 and optimized using the simulat-

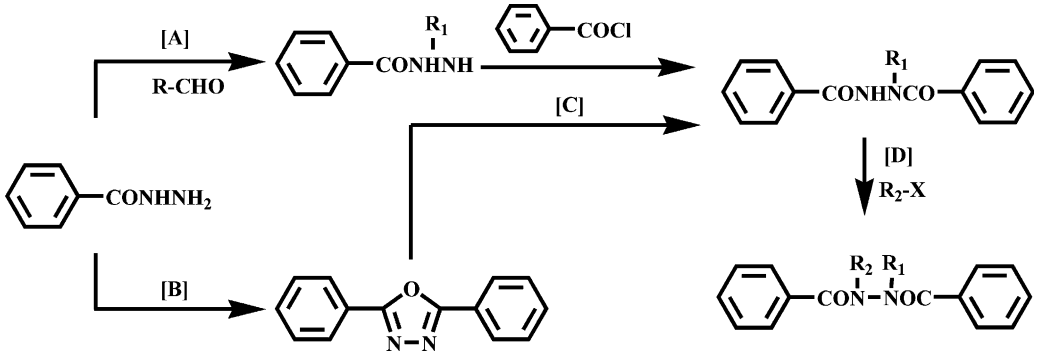

Scheme 2. Alternative synthesis methods for dibenzoylhydrazine derivatives using benzoylhydrazine and the corresponding alkyl halide. The experimental procedures for pathways A–D are described in the text.

Table 4. Melting points and elemental analyses of newly synthesized compounds[a]

Compound	Mp (°C)	Elemental analyses
111	228–230	Found: C, 75.75; H, 8.47; N, 7.40 Calcd: C, 75.75; H, 8.48; N, 7.36
114	214	Found: C, 64.15; H, 6.02; N, 7.12 Calcd: C, 64.28; H, 5.91; N, 7.14
119	242–243	Found: C, 63.38; H, 5.55; N, 7.54 Calcd: C, 63.48; H, 5.59; N, 7.40
120	239	Found: C, 63.40; H, 5.61; N, 7.37 Calcd: C, 63.48; H, 5.59; N, 7.40
123	239–242	Found: C, 48.70; H, 4.31; N, 6.02 Calcd: C, 48.74; H, 4.31; N, 5.98
126	214–215	Found: C, 43.49; H, 3.40; N, 8.30 Calcd: C, 43.31; H, 3.43; N, 8.42
127	201–203	Found: C, 73.80; H, 7.39; N, 8.63 Calcd: C, 74.04; H, 7.46; N, 8.64
128	249–250	Found: C, 58.97; H, 5.02; N, 7.54 Calcd: C, 59.19; H, 4.97; N, 7.67
129	246–247	Found: C, 66.10; H, 6.27; N, 8.13 Calcd: C, 66.18; H, 6.14; N, 8.12
130	180–182	Found: C, 74.70; H, 8.12; N, 8.18 Calcd: C, 74.97; H, 8.01; N, 7.95
131	249	Found: C, 58.68; H, 4.51; N, 7.63 Calcd: C, 58.94; H, 4.67; N, 7.64
134	213–214	Found: C, 71.25; H, 8.55; N, 9.31 Calcd: C, 71.49; H, 8.67; N, 9.26
135	87–88	Found: C, 71.12; H, 9.27; N, 9.19 Calcd: C, 71.02; H, 9.27; N, 9.20
136	151–153	Found: C, 71.66; H, 9.57; N, 8.81 Calcd: C, 71.66; H, 9.50; N, 8.80
137	161–162	Found: C, 71.56; H, 9.24; N, 8.83 Calcd: C, 71.66; H, 9.50; N, 8.80
138	159–160	Found: C, 71.98; H, 9.73; N, 8.45 Calcd: C, 72.25; H, 9.70; N, 8.43
139	112–113	Found: C, 72.65; H, 9.92; N, 8.06 Calcd: C, 72.79; H, 9.89; N, 8.08
140	209–210	Found: C, 70.25; H, 9.21; N, 9.86 Calcd: C, 70.31; H, 9.02; N, 9.66
155	145–146	Found: C, 70.84; H, 5.47; N, 11.06 Calcd: C, 70.85; H, 5.55; N, 11.02
156	127–128	Found: C, 71.58; H, 5.96; N, 10.38 Calcd: C, 71.62; H, 6.01; N, 10.44
157	164–165	Found: C, 72.20; H, 6.46; N, 9.96 Calcd: C, 72.32; H, 6.43; N, 9.92
158	103–104	Found: C, 72.88; H, 6.87; N, 9.44 Calcd: C, 72.95; H, 6.80; N, 9.45
159	171–173	Found: C, 72.98; H, 6.78; N, 9.52 Calcd: C, 72.95; H, 6.80; N, 9.45
160	167–170	Found: C, 72.91; H, 6.80; N, 9.53 Calcd: C, 72.95; H, 6.80; N, 9.45
161	167–168	Found: C, 73.67; H, 7.14; N, 9.01 Calcd: C, 73.52; H, 7.14; N, 9.03
162	161–162	Found: C, 73.62; H, 7.14; N, 9.12 Calcd: C, 73.52; H, 7.14; N, 9.03
163	178–179	Found: C, 75.77; H, 5.23; N, 8.84 Calcd: C, 75.93; H, 5.10; N, 8.86
164	173	Found: C, 71.87; H, 4.59; N, 8.40 Calcd: C, 71.85; H, 4.52; N, 8.38
165	199–201	Found: C, 74.52; H, 6.93; N, 8.70 Calcd: C, 74.51; H, 6.88; N, 8.69
166	200–201	Found: C, 74.98; H, 7.26; N, 8.33 Calcd: C, 74.97; H, 7.19; N, 8.33
167	71–72	Found: C, 71.59; H, 5.93; N, 10.44 Calcd: C, 71.62; H, 6.01; N, 10.44
168	119–121	Found: C, 73.27; H, 7.15; N, 9.00 Calcd: C, 73.52; H, 7.14; N, 9.03
169	53–56	Found: C, 74.95; H, 7.92; N, 7.98
170	107–109	Calcd: C, 74.97; H, 8.01; N, 7.95 Found: C, 75.32; H, 8.26; N, 7.46 Calcd: C, 75.38; H, 8.25; N, 7.64

[a] Analyses were performed at the Center for Organic Elemental Microanalysis of Kyoto University. Mp = melting point.

ed annealing method. To optimize the protein structure, the original DBH-type ligand (BYI06830) in 1R20 was used as a ligand. The coordinates of BYI06830 were fixed during optimization.

The cavity surface at the ligand-binding site of the modeled BmEcR was expressed by the MOLCAD module of SYBYL using the Fast Conolly algorithm. The gradient of the hydrophobic property of the cavity surface was colored from blue (less hydrophobic) to brown (more hydrophobic) in Figure 8 based on the approach by Heiden et al.[52]

5.4. Synthesis of compounds

N-*tert*-Butyl-*N*,*N*′-dibenzoylhydrazines were synthesized with a range of substituents on the benzene rings using *tert*-butylhydrazine and benzoyl chloride according to previously published methods (Schemes 1 and 2; Table 4). Substituted benzoyl chloride was prepared from the corresponding benzoic acid and arylhydrazines were used to introduce aryl groups on the *N*-atom. 4-Fluorophenylhydrazine was derived from 4-fluoroaniline according to the conventional method.[53] As hydrazine compounds are explosive, sufficient caution must be used in their handling, and particular attention must be paid to avoid condensation. Other dibenzoylhydrazine derivatives containing various alkyl groups on the *N*-atoms were synthesized according to the procedures shown in Scheme 2. Introduction of primary and secondary alkyl groups was executed by reacting benzoylhydrazine (benzoic hydrazide) and the corresponding alkyl halide. A *tert*-amyl group was introduced by reaction of the corresponding *tert*-amyl carbocation with 2,5-diphenyl-1,3,4-oxazole derived from two benzoylhydrazine molecules. The ^{1}H NMR spectra were recorded on a JEOL JNM-PMX60 (Tokyo, Japan) spectrometer with the use of $CDCl_3$ and/or deuteriodimethylsulfoxide (DMSO-d_6) with tetramethylsilane (TMS) as the internal standard. Experimental procedures for steps A–D in Scheme 2 are described below.

5.5. *N*-Benzoyl-*N*′-*n*-butylhydrazine (step A)

N-Benzoylhydrazine (1.36 g, 10.0 mmol) and *n*-butyraldehyde (0.72 g, 10.0 mmol) in methanol (30 ml) with a catalytic amount of *para*-toluenesulfonic acid were stirred overnight to obtain the corresponding hydrazone. To the reaction mixture was added $NaBH_3CN$ (0.75 g, 12 mmol) with the simultaneous addition of 4 M HCl in dioxane to keep the mixture acidic and stirred for 3 h at room temperature. After stripping of the organic solvents under reduced pressure, water was added to the

residue followed by extraction with ether. The ether layer was dried over anhydrous Na_2SO_4 and concentrated in vacuo to obtain a yellow oil containing *N*-benzoyl-*N*′-*n*-butylhydrazine (0.80 g), which was purified by silica gel column (Walogel C-300) chromatography (hexane/ethyl acetate = 2/1). ^{1}H NMR ($CDCl_3$) δ 0.90 (3H, t, J = 7 Hz), 1.48 (6H, m), 2.00 (1H, s), 6.00–7.00 (1H, br), 7.20–7.90 (5H, m).

5.6. 2,5-Diphenyl-1,3,4-oxadiazole (step B)

Benzoic hydrazide (benzoylhydrazine, 5.00 g, 36.8 mmol) was dissolved in polyphospholic acid (100 g) and stirred for 40 min at 170 °C. After cooling, the reaction mixture was poured into water. The solid material was filtered and washed with water, and then crystallized from ethanol to obtain 2,5-diphenyl-1,3,4-oxadiazole (3.20 g, 78.0%). ^{1}H NMR ($CDCl_3$) δ 7.00–7.60 (10H, mj).

5.7. *N*,*N*′-Dibenzoyl-*N*′-*tert*-amylhydrazine (step C)

2,5-Diphenyl-1,3,4-oxadiazole (1.11 g, 5.0 mmol) was dissolved in 2-methyl-2-butene (1.40 g, 10.0 mmol) and concentrated H_2SO_4 (0.98 g, 10.0 mmol) and stirred for three days. After the addition of water, the mixture was extracted with ether. The ether layer was washed with saturated $NaHCO_3$, followed by brine and then dried over anhydrous Na_2SO_4. The solvent was stripped under reduced pressure and the residue was purified by silica gel chromatography (hexane/ethyl acetate = 2/1) to afford *N*,*N*′-dibenzoyl-*N*′-*tert*-amylhydrazine as a colorless oil. ^{1}H NMR ($CDCl_3$) δ 0.92 (3H, t, J = 7 Hz), 1.30–2.00 (6H, m), 7.00–7.60 (10H, m), 9.80 (1H, s).

5.8. *N*,*N*′-Dibenzoyl-*N*-*n*-butyl-*N*′-*tert*-butylhydrazine (step D)

N,*N*′-Dibenzoyl-*N*′-*tert*-butylhydrazine was prepared according to the conventional method by the gradual addition of NaH (0.20 g) to 20 ml of *N*,*N*-dimethylformamide (DMF) followed by stirring for 30 min. Next, *n*-butyl iodide (0.74 g, 4.0 mmol) was added dropwise to the mixture and stirred for 2 h at room temperature. The reaction mixture was diluted with 50 ml of water, extracted with ether and the organic layer was washed with 1 M HCl and brine, and then dried over anhydrous Na_2SO_4. After stripping the solvent, the residue was purified by silica gel column chromatography to give *N*,*N*′-dibenzoyl-*N*-*n*-butyl-*N*′-*tert*-butylhydrazine as a yellowish oil. ^{1}H NMR ($CDCl_3$) δ 0.90 (3H, t, J = 7 Hz), 1.00–1.50 (4H, m), 1.66 (9H, s), 3.05–3.40 (2H, J = 8 Hz, t), 7.20–7.70 (10H, br s).

Acknowledgments

Craig E. Wheelock was funded by a Japanese Society for the Promotion of Science (JSPS) postdoctoral fellowship. Guy Smagghe acknowledges the Fund for Scientific Research (FWO-Vlaanderen, Brussels, Belgium). Dimitra Stefanou, Kostas Iatrou and Luc Swevers acknowledge the support of the General Secretariat of Science and Technology, Greek Ministry of Development. This study was supported, in a part, by the 21st century COE program for Innovative Food and Environmental Studies Pioneered by Entomomimetic Sciences, from the Ministry of Education, Culture, Sports, Science and Technology of Japan. The authors thank Åsa Wheelock for assistance with the CoMFA figures.

References and notes

1. Nijhout, H. F. *Insect Hormones*; Princeton University Press: New Jersey, 1994.
2. Yao, T.-P.; Segraves, W. A.; Oro, A. E.; McKeown, M.; Evans, R. M. *Cell* **1992**, *71*, 63.
3. Thomas, H. E.; Stunnenberg, H. G.; Stewart, A. F. *Nature* **1993**, *362*, 471.
4. Yao, T.-P.; Forman, B. M.; Jiang, Z.; Cherbas, L.; Chen, J.-D.; McKeown, M.; Cherbas, P.; Evans, R. M. *Nature* **1993**, *366*, 476.
5. Hsu, A. C. -T. In *Synthesis and Chemistry of Agrochemicals II*; Baker, D. R., Fenyes, J. G., Moberg, W. K., Eds.; American Chemical Society: Washington, DC, 1991; Vol. 443, p.478.
6. Dhadialla, T. S.; Carlson, G. R.; Le, D. P. *Annu. Rev. Entomol.* **1998**, *43*, 545.
7. Sawada, Y.; Yanai, T.; Nakagawa, H.; Tsukamoto, Y.; Tamagawa, Y.; Yokoi, S.; Yanagi, M.; Toya, T.; Sugizaki, H.; Kato, Y.; Shirakura, H.; Watanabe, T.; Yajima, Y.; Kodama, S.; Masui, A. *Pest Manag. Sci.* **2003**, *59*, 49.
8. Sawada, Y.; Yanai, T.; Nakagawa, H.; Tsukamoto, Y.; Yokoi, S.; Yanagi, M.; Toya, T.; Sugizaki, H.; Kato, Y.; Shirakura, H.; Watanabe, T.; Yajima, Y.; Kodama, S.; Masui, A. *Pest Manag. Sci.* **2003**, *59*, 25.
9. Sawada, Y.; Yanai, T.; Nakagawa, H.; Tsukamoto, Y.; Yokoi, S.; Yanagi, M.; Toya, T.; Sugizaki, H.; Kato, Y.; Shirakura, H.; Watanabe, T.; Yajima, Y.; Kodama, S.; Masui, A. *Pest Manag. Sci.* **2003**, *59*, 36.
10. Henrich, V. C. In *Comprehensive Molecular Insect Science*; Gilbert, L. I., Iatrou, K., Gill, S. S., Eds.; Elsevier: Oxford, 2005; p 243.
11. Laudet, V.; Bonneton, F. In *Comprehensive Molecular Insect Science*; Gilbert, L. I., Iatrou, K., Gill, S. S., Eds.; Elsevier: Oxford, 2005; p 287.
12. Wing, K. D. *Science* **1988**, *241*, 467.
13. Wing, K. D.; Slawecki, R. A.; Carlson, G. R. *Science* **1988**, *241*, 470.
14. Nakagawa, Y.; Akagi, T.; Iwamura, H.; Fujita, T. *Pestic. Biochem. Physiol.* **1989**, *33*, 144.
15. Nakagawa, Y.; Shimizu, B.; Oikawa, N.; Akamatsu, M.; Nishimura, K.; Kurihara, N.; Ueno, T.; Fujita, T. In *Classical and Three-Dimensional QSAR in Agrochemistry*; Hansch, C., Fujita, T., Eds.; American Chemical Society: Washington, DC, 1995; Vol. 606; p 288.
16. Nakagawa, Y.; Hattori, K.; Shimizu, B.; Akamatsu, M.; Miyagawa, H.; Ueno, T. *Pestic. Sci.* **1998**, *53*, 267.
17. Nakagawa, Y.; Hattori, K.; Minakuchi, C.; Kugimiya, S.; Ueno, T. *Steroids* **2000**, *65*, 117.
18. Nakagawa, Y.; Minakuchi, C.; Ueno, T. *Steroids* **2000**, *65*, 537.
19. Nakagawa, Y.; Minakuchi, C.; Takahashi, K.; Ueno, T. *Insect Biochem. Mol. Biol.* **2002**, *32*, 175.
20. Nakagawa, Y.; Smagghe, G.; Tirry, L.; Fujita, T. *Pest Manag. Sci.* **2002**, *58*, 131.
21. Nakagawa, Y.; Takahashi, K.; Kishikawa, H.; Ogura, T.; Minakuchi, C.; Miyagawa, H. *Bioorg. Med. Chem.* **2005**, *13*, 1333.

22. Smagghe, G.; Degheele, D. *Pestic. Biochem. Physiol.* **1994**, *49*, 224.
23. Hsu, A. C.-T; Fujimoto, T. T.; Dhadialla, T. S. In *Phytochemicals for Pest Control*; Hedin, P. A., Hollingworth, R. M., Masler, E. P., Miyamoto, J., Thompson, D. G., Eds.; American Chemical Society: Washington, DC, 1997; p 206.
24. Carlson, G. R. In *Green Chemical Syntheses and Processes*; Anastas, P. T., Heine, L. G., Williamson, T. C., Eds.; American Chemical Society: Washington, DC, 2000; Vol. 767, p 8.
25. Trisyono, A.; Chippendale, M. *J. Econ. Entomol.* **1997**, *90*, 1486.
26. Trisyono, A.; Chippendale, M. *Pestic. Sci.* **1998**, *53*, 177.
27. Carlson, G. R.; Dhadialla, T. S.; Hunter, R.; Jansson, R. K.; Jany, C. S.; Lidert, Z.; Slawecki, R. A. *Pest Manag. Sci.* **2001**, *57*, 115.
28. Cowles, R. S.; Alm, S. R.; Villani, M. G. *J. Econ. Entomol.* **1999**, *92*, 427.
29. Farinos, G. P.; Smagghe, G.; Tirry, L.; Castanera, P. *Arch. Insect Biochem. Physiol.* **1999**, *41*, 201.
30. Smagghe, G.; Degheele, D. *Pestic. Biochem. Physiol.* **1993**, *46*, 149.
31. Smagghe, G.; Nakagawa, Y.; Carton, B.; Mourad, A. K.; Fujita, T.; Tirry, L. *Arch. Insect Biochem. Physiol.* **1999**, *41*, 42.
32. Elzen, G. W. *J. Econ. Entomol.* **2001**, *94*, 55.
33. Le, D. P.; Thirugnanam, M.; Lidert, Z.; Carlson, G. R.; Ryan, J. B. *Proc. Brighton Crop Prot. Conf.—Pests Dis.* **1996**, 481.
34. Billas, I. M. L.; Iwema, T.; Garnier, J. M.; Mitschler, A.; Rochel, N.; Moras, D. *Nature* **2003**, *426*, 91.
35. Swevers, L.; Kravariti, L.; Ciolfi, S.; Xenou-Kokoletsi, M.; Ragoussis, N.; Smagghe, G.; Nakagawa, Y.; Mazomenos, B.; Iatrou, K. *FASEB J.* **2004**, *18*, 134.
36. Toya, T.; Yamaguchi, K.; Endo, Y. *Bioorg. Med. Chem.* **2002**, *10*, 953.
37. Nakagawa, Y.; Takahashi, K.; Kishikawa, H.; Ogura, T.; Minakuchi, C.; Miyagawa, H. *Bioorg. Med. Chem.* **2005**, *13*, 1333.
38. Klebe, G.; Abraham, U.; Mietzner, T. *J. Med. Chem.* **1994**, *37*, 4130.
39. Carmichael, J. A.; Lawrence, M. C.; Graham, L. D.; Pilling, P. A.; Epa, V. C.; Noyce, L.; Lovrecz, G.; Winkler, D. A.; Pawlak-Skrzecz, A.; Eaton, R. E.; Hannan, G. N.; Hill, R. J. *J. Biol. Chem.* **2005**, *280*, 22258.
40. Ogura, T.; Nakagawa, Y.; Minakuchi, C.; Miyagawa, H. *J. Pestic. Sci.* **2005**, *30*, 1.
41. Wheelock, C. E.; Nakagawa, Y.; Akamatsu, M.; Hammock, B. D. *Bioorg. Med. Chem.* **2003**, *11*, 5101.
42. Oikawa, N.; Nakagawa, Y.; Nishimura, K.; Ueno, T.; Fujita, T. *Pestic. Biochem. Physiol.* **1994**, *48*, 135.
43. Oikawa, N.; Nakagawa, Y.; Nishimura, K.; Ueno, T.; Fujita, T. *Pestic. Sci.* **1994**, *41*, 139.
44. Fleischer, R.; Wiese, M. *J. Med. Chem.* **2003**, *46*, 4988.
45. Hansch, C.; Leo, A. J.; Hoekman, D. *Exploring QSAR: Hydrophobic, Electronic, and Steric Constants*; American Chemical Society: Washington, DC, 1995.
46. Asao, M.; Shimizu, R.; Nakao, K.; Fujita, T. *Japan Chemistry Program Exchange*; Society of Computer Chemistry: Japan, 1997.
47. Leo, A. J. *Chem. Rev.* **1993**, *93*, 1281.
48. Cramer, R. D., III *Perspect. Drug Discov. Des.* **1993**, *1*, 269.
49. Ogata, K.; Umeyama, H. *J. Mol. Graph. Model.* **2000**, *18*, 258.
50. Swevers, L.; Drevet, J. R.; Lunke, M. D.; Iatrou, K. *Insect Biochem. Mol. Biol.* **1995**, *25*, 857.
51. Kamimura, M.; Tomita, S.; Fujiwara, H. *Comp. Biochem. Physiol. B* **1996**, *113*, 341.
52. Heiden, W.; Moeckel, G.; Brickmann, J. J. *Comput. Aided Mol. Des.* **1993**, *7*, 503.
53. Coleman, G. H. In *Organic Synthesis Collection*; Gilman, H., Eds.; Wiley: New York, 1967; Vol. 1, p 442.
54. Nakagawa, Y.; Smagghe, G.; Kugimiya, S.; Hattori, K.; Ueno, T.; Tirry, L.; Fujita, T. *Pestic. Sci.* **1999**, *55*, 909.